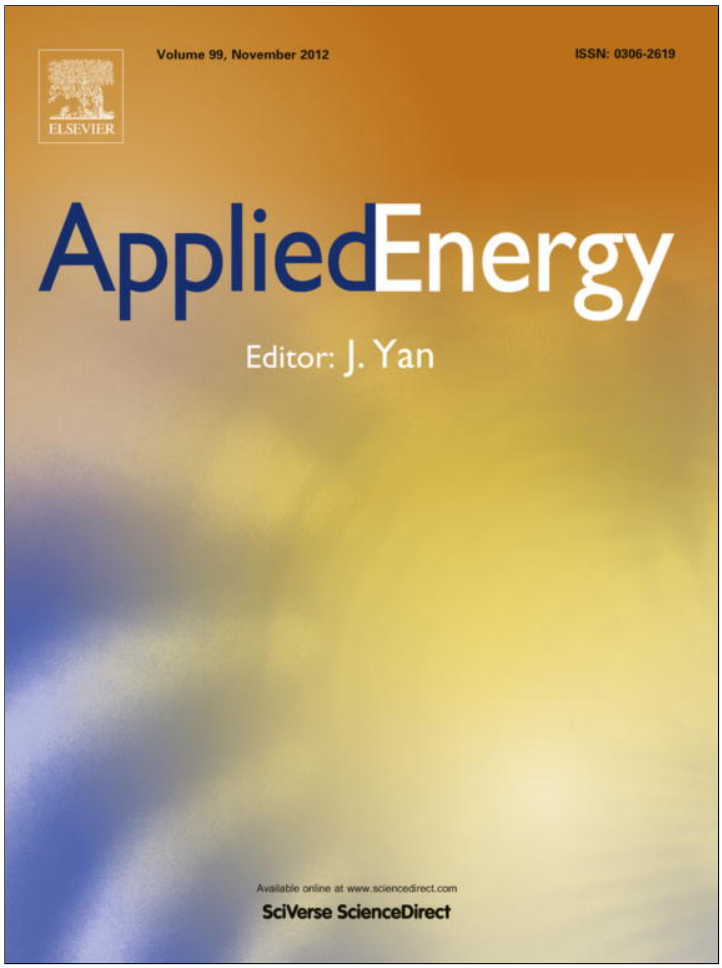

Applied Energy 99 (2012) 255–264

Contents lists available at SciVerse ScienceDirect

Applied Energy

journal homepage: www.elsevier.com/locate/apenergy

Optimal sensor placement in integrated gasification combined cycle power systems

Adrian J. Lee, Urmila M. Diwekar *

Center for Uncertain Systems, Tools for Optimization and Management, Vishwamitra Research Institute, Clarendon Hills, IL 60514, USA

HIGHLIGHTS

- Addresses the sensor placement problem in advanced power system.
- Presents the problem as a stochastic programming problem.
- Considers fisher information based objectives along with the economics of sensor.
- For the first time addresses the problem of sensor placement in advanced power systems.

ARTICLE INFO

Article history:
Received 25 October 2011
Received in revised form 14 March 2012
Accepted 16 April 2012
Available online 15 June 2012

Keywords:
Sensor placement
IGCC power plant
Sensor variability
Fisher information
Stochastic optimization

ABSTRACT

The optimal sensor placement problem involves determining the most effective locations to place a network of sensors across an array of measurable signals, in accordance with a set of specified objectives and constraints, such as cost, performance, and sensitivity to variations in uncertain environments. In advanced power systems, such as in pulverized coal and integrated gasification combined cycle power plants, the placement of sensors on-line within the power generation process can be expensive or technically infeasible due to certain harsh environments. This paper uses advanced modeling techniques to simulate the system's steady state behavior, and to capture the variability in unknown process variables using the accuracy information from a given set of online sensors. This variability and measurement error is analyzed using a technique from information theory to determine the most cost-effective network of on-line sensors by formulating a nonlinear, stochastic binary integer problem. The solution is achieved by using an efficient sampling technique, Better Optimization algorithm for Nonlinear Uncertain Systems. The key contribution of using Fisher information as a metric for observation order is that it generalizes the Gaussian assumption on representing process and measurement variability for systems governed by nonlinear dynamics.

1. Introduction

The sensor placement problem typically refers to the determination of the optimal network of sensors placed within a system containing multiple measurable signals, given a set of cost and performance constraints. The sensor placement problem can be defined so as to either minimize the number of sensors or overall sensor cost, or to maximize reliability or accuracy, for example, given a set of performance constraints [1–3]. Moreover, the sensor network may take into consideration the cost versus benefits of sensor inclusion (exclusion) within fault detection or control software algorithms [4–6]. In advanced power systems, such as in Pulverized Coal (PC) and Integrated Gasification Combined Cycle (IGCC) power plants, sensors can be placed on input, intermediate, and output signals to monitor the evolution of the process variables within the power generation process. However, placing a sensor to measure each and every one of these process variables can be either expensive or technically infeasible within certain harsh environments.

Through advanced modeling techniques, it is possible to closely simulate the behavior of the power system [7–9]. This plays a particularly important role when considering the high levels of measurement uncertainty that exist within sensors subjected to harsh environments. By introducing variability into several process inputs, it is possible to simulate the resulting variance of the downstream variables. This variability and sensor accuracy is then analyzed using techniques from information theory to determine which signals can be observed using *virtual* sensors (i.e., process variables estimated using simulation software), and which should be measured using a network of *on-line* sensors (i.e., sensors physically placed in the plant environment). First, the IGCC process utilized in this paper is outlined. Then, the contribution of this paper and related work is described to address the problem of deploying sensors in an environment exhibiting high measurement uncertainty.

* Corresponding author.
E-mail address: urmila@vri-custom.org (U.M. Diwekar).

0306-2619/$ - see front matter © 2012 Elsevier Ltd. All rights reserved.
http://dx.doi.org/10.1016/j.apenergy.2012.04.027

1.1. IGCC process

Advanced power generation systems, such as the Tampa Electric Company Polk power station IGCC plant located in Polk County, Tampa, Florida, for example, consist of numerous process variables, including temperature, pressure, and flow rate of steam, oxygen, carbon dioxide, and other byproduct gases, liquids and solids. The Tampa IGCC power plant uses an oxygen-blown, entrained flow coal gasifier to produce a synthesis gas, called syngas, which is then used to fuel an advanced combustion turbine [10]. Fig. 1 illustrates a simplified process flowchart of the IGCC plant [11]. The main elements of the power plant include the air separation unit (ASU), the gasification plant, and the power block. The ASU separates ambient air into oxygen (O_2) (at 96% purity) and nitrogen (N_2). Most of the oxygen is used to produce fuel gas in the gasification plant, while most of the nitrogen is used to dilute fuel gas and reduce nitrous oxide (NO_x) levels in the power plant's combustion turbine.

The gasification plant converts coal or other solid fuel (i.e., petroleum coke or biomass) into fuel gas and high pressure steam by reacting with the O_2 from the ASU, which is then used to produce electricity within high and low pressure gas and steam turbines. The subsections of the gasification plant include coal receiving and storage, slurry preparation, gasification and high temperature heat recovery, slag and process water handling, gas cleaning, and sulfur recovery. Prior to entering the gasifier, coal fines are mixed with water and ground into a viscous slurry. The gasifier typically operates at a temperature and pressure around 1645 K and 2760 KPa, where the coal slurry and oxygen react in the gasifier to produce syngas, slag, and flyash. Syngas is composed of mainly hydrogen (H_2), water vapor (H_2O), carbon monoxide (CO), and carbon dioxide (CO_2), while smaller amounts of hydrogen sulfide (H_2S), carbonyl sulfide (COS), methane (CH_4), argon (Ar), nitrogen (N_2), and ammonia (NH_3) are also produced. Slag is a mineral matter and byproduct of the gasification process, resulting from the remainder of coal that does not convert to syngas. The slag flows down the gasifier walls, solidifies into an inert glassy frit with little carbon content, and is removed from the process as waste. Flyash is partially gasified residual carbon (i.e.,"char"), which exits the gasifier within the syngas stream. High pressure steam is produced by first cooling the syngas in a radiant syngas cooler (RSC), then passing through a high pressure steam generator and gas cooler. The RSC is used to help improve efficiency and reliability, as opposed to using a water quenching process [12]. In addition, efficiency may be improved by employing hot gas desulfurization to reduce nitrous oxide (NO_x) emissions [13]. An intensive water scrubbing step is used to help remove particulate matter, including flyash, contained in the syngas. In addition, the COS is converted to H_2S to be easily removed from the syngas, while the NO_x is removed from the process by using a Selective Catalytic Reduction technique.

Lastly, the power block subsection consists of a series of combustion turbines that generate electricity from fuel gas, nitrogen, and high pressure steam. A heat recovery steam generator (HRSG) uses the gas turbine exhaust gas to preheat boiler feedwater and generate both high and low pressure steam, while also reheating all the plant's steam for powering a series of high, intermediate, and low pressure steam turbines. To help reduce the environmental impacts resulting from the power generation process, the IGCC plant also utilizes a gas clean-up system and a high efficiency combined cycle to help lower SO_2, NO_x, and particulate levels. The model used for IGCC in this work is taken from the DOE/NETL Case study 8 report [11]. Variations on the IGCC process include the use of an air-blown gasifier for improved thermodynamic performance instead of the oxygen-blown gasifier used in the Polk power station [14].

1.2. Measurement uncertainty

Variations to certain input process variables, such as slurry and oxygen mass-flow rates, can lead directly to variations in the gasification performance. For example, adjustments made to the coal slurry flow rate alter the syngas header pressure, while adjustments made to the ratio of oxygen to coal slurry can alter the gasifier operating temperature. Due to the harsh environments that exist within the gasifier (i.e. extreme temperature and pressure), knowing the true gasifier temperature and choosing an appropriate target operating point become difficult tasks. Controlling the gasification process at the optimal temperature is essential since refractory wear rate worsens at higher operating temperatures, while the gasifier produces excessive amount of flyash for lower operating temperatures. Lower temperature also results in higher unconverted carbon, which ends up in slag. In addition, abrasion and erosion corrosion occurs at elevated temperatures and pressures. Syngas also has a direct impact on the operating conditions within the gas turbine and its interaction with the ASU [15,16]. Possible methods for monitoring the gasifier temperature include both direct and indirect measurements [17,18]. Unfortunately, standard thermocouples cannot be used to provide a temperature

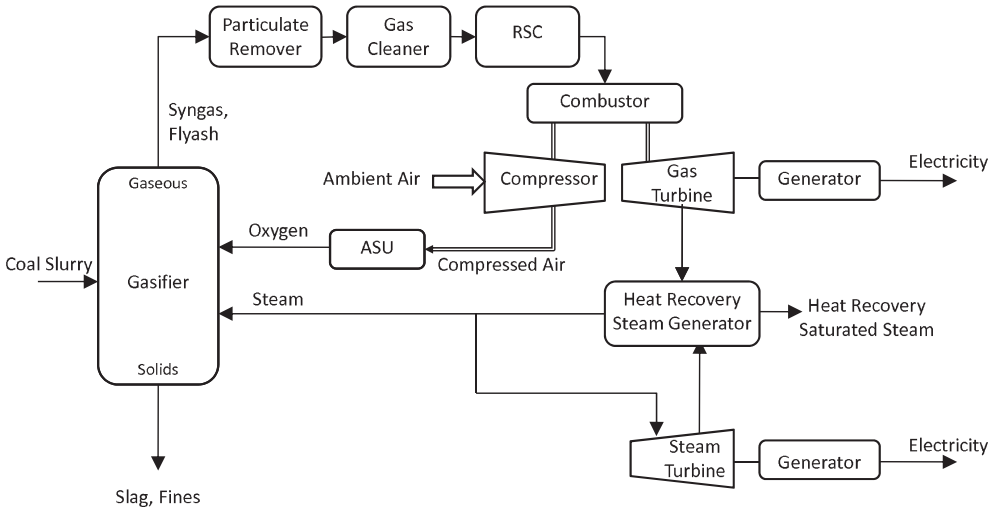

Fig. 1. Simplified IGCC process.

measurement directly within the gasifier flow path. Instead, inferential measurements are currently made based on the measurements obtained from related process variables. For example, the rate at which methane is formed depends on both the gasifier temperature and the fuel composition. Since the fuel composition depends upon the temperature and reactivity of the fuel and slag components, the gasifier temperature may be estimated by measuring the methane production and by monitoring the appropriate fuel and slag properties [10].

Monitoring all the process variables contained in the IGCC plant operations using a complete network of sensors would prove to be both costly and, in some cases, technically infeasible due to the inability to obtain measurements within harsh environments. Instead, several of these process variables may be estimated, rather than directly measured, by inferring their values through measurements obtained from related process variables. At this time, there exists only limited research pertaining to the optimal placement of sensors in IGCC plants in literature. However, a vast amount of effort has been devoted to optimizing sensor placement in the measurement of chemical processes. Ali and Narasimhan [1] present a method for determining the optimal location of sensors in a steady-state process by maximizing the reliability of the sensor measurements, by maximizing the probability of estimating the system variables in the presence of sensor failure. Alonso et al. [2] use a reduced order, linear dynamical model of a chemical reactor to determine the location, number, and type of sensors to deploy through a min–max optimization problem.

There does, however, exist numerous contributions to the problem of sensor location for state estimation. Within these contributions, several measures have been defined to determine a system's optimal sensor network. Optimality criteria based on the error covariance matrix [19–23], and observability matrix or Gramian [24,25] are commonly used. In addition, there are contributions that account for measurement cost, sensor failure, and redundancy in addition to process information [26–29] . For example, Bagajewicz [30] and Chmielewski et al. [3] present techniques related to the minimization of cost, subject to constraints related to data reconciliation, while Muske and Georgakis [31] present a sensor location technique that provides the best compromise between measurement cost and process information – each of which are restricted to linear systems. There exist research in sensor placement that addresses nonlinear systems but these approaches are derived from a linearization of the systems and are limited to low order systems [32–34]. On the other hand, most of optimality criteria for the parameter estimation when the sensor location is fixed is based on scalar measures of Fisher information and are based on local sensitivity information [35–37].

In an effort to reduce the overall purchase costs associated with deploying a network of on-line sensors, this paper defines a sensor placement problem for advanced power systems, where the objective is to find the optimum location of sensors, subject to specified cost constraints. To capture the amount of variability in the process for a given network of sensors, this paper presents the novel use of Fisher information as a metric of observation order, by capturing the amount of information contained in a set of observations. Moreover, the underlying contribution of this paper is to use Fisher information to quantify the level of uncertainty in the set of on-line and virtual sensors, thereby aiding in determining the optimal deployment of a sensor network given cost constraints. An advanced model of the IGCC power plant, developed in the ASPEN Plus simulation environment, is used to quantify the variability of downstream process variables as a result of variability in a set of input process variables, including coal and oxygen flow rates, gasifier temperature, and gasifier pressure. Using the known measurement distributions of the sensors placed online in the plant, the Fisher information can then be evaluated at the unmeasured locations. This quantity is then used within the objective function to determine which of the downstream process variables should be observed or physically measured through the placement of candidate sensors. The key benefit from this approach is that Fisher information can be used to address processes that exhibit nonlinear interactions among the system variables, while also accommodating non-Gaussian system and measurement noise.

This paper is organized as follows: Section 2 provides a background on Fisher information and its relevancy to the sensor placement problem. Section 3 then formulates the sensor placement problem as a nonlinear, stochastic binary integer program. Section 4 provides computational results illustrating the use of Fisher information to determine the optimal deployment of a network of sensors in an IGCC power plant, while Section 5 provides concluding remarks and future directions.

2. Fisher information background

Fisher information is a statistical measure established in the field of information theory, and named after the work by Ronald Fisher [38]. For a set of independent and identically distributed observations, $x_1, x_2, \ldots, x_n$, resulting from n outcomes of a random variable, $X = X_i$, $i = 1, 2, \ldots, n$, various statistical measures can be used to capture the amount of information that the set of observations contains about the distribution properties of X, including Shannon information, Boltzmann–Gibbs, Tsallis, Renyi, and Sharma–Mittal entropies, among others [39]. Fisher information, however, has a unique property capturing the amount of information the observations, $x_1, x_2, \ldots, x_n$, contains about some unknown parameter, θ_x, within the distribution, $p_X(x)$, such as its expectation or variance, for example, by quantifying the *expected change* in the distribution due to a change in this parameter value. One expression for Fisher information, $I_X(\theta_x)$, is given by [40]

$$I_X(\theta_x) = E^X\left[\left(\frac{1}{p_{X|\Theta_x}(x|\theta_x)}\frac{\partial p_{X|\Theta_x}(x|\theta_x)}{\partial \theta_x}\right)^2\right], \tag{1}$$

where the distribution $p(x|\theta_x)$ is the likelihood of x, given the parameter θ_x. Several alternative forms of (1) exist, such as the shift-invariant, tensor, multi-parameter, and amplitude q-form [40]. For example, the shift-invariant form of (1) occurs when the shape of the distribution of X remains unchanged from a shift in the parameter θ_x (i.e., the uniform and normal distributions resulting from a shift in the mean value). In addition, Fisher information satisfies the Cramer–Rao inequality, $e^2 I_X(\theta_x) \geqslant 1$, where e^2 is the mean squared error [40]. Moreover, equality holds for efficient, unbiased estimators, and the Fisher information becomes equal to the inverse of the variance of X (i.e., $I_X(\theta_x) = 1/Var(X)$).

Fisher information is also viewed as a statistical measure of dynamic system order that quantifies the variability in a process variable as a function of changes in the mean value of the governing distribution. This property serves well as a measure of the order in a set of observations (i.e., the level of observation order), where a shift in the variability in a set of measurements directly affects the *ability* to estimate the unknown state of the variable due to the partial derivative in (1). Note that the unknown state can also be identified as locally observable (or unobservable) through the Fisher information matrix [41], in the sense that the state can (not) in fact be estimated. It is a suitable metric for the sensor placement problem mainly due to its local property. In practice, the true value of a process variable undergoes changes with respect to time, producing a corresponding mean value shift in the sensor measurement distribution. Due to the gradient operator, $\partial/\partial\theta_x$, Fisher information measures the amount of change in the likelihood function due to a change in the unknown parameter

value. Lower (higher) Fisher information values indicate that $p(x|\theta_x)$ changes slower (faster) with respect to a change in θ_x, and hence, corresponds to a lower (higher) level of observation order in regards to estimating the true parameter value.

Fisher information has been introduced in literature as a metric for quantifying the sustainability of ecological systems [42–45], for determination of optimal spacial locations of sensors [36], and in financial applications [46], among others. Several expressions for obtaining Fisher information have been derived [40], including a time-dependent expression for quantifying changes in Lotka–Volterra cyclic behavior and the determination of ecological regime shifts [42].

For the sensor placement problem, the objective is to maximize the overall observation order of the system, subject to constraints associated with the purchase, deployment, and maintenance of a network of on-line sensors. Thus, the goal is to decrease the overall sensor cost by determining the optimal sensor locations which maximize the amount of information pertaining to the true state of the system. Note that while the information gathered from the set of observations can ultimately lead to state estimation, the determination of the sensor network only relies on maximizing an overall Fisher information quantity based on the measurement distributions across all sensor nodes. As part of a stochastic optimization problem, the decision to either observe or measure each process variable results from the uncertainty surrounding the true values of the process variables in the form of system and measurement noise. By determining the placement of sensors over all measurable process variables using Fisher information as a metric for optimization, the overall number of sensors can also be decreased, thereby producing a more cost-effective solution to monitoring the power system.

From the Cramer–Rao inequality, Fisher information is related to the inverse of the variance, and hence, can indicate similar characteristics of system accuracy to sensor placement using data reconciliation [47–49]. In comparison, data reconciliation is based on minimizing the penalty of sensor measurements, and is also related to the measurement variance (weighted by the standard deviation of the set of measurements). However, Fisher information as a metric allows one to determine the placement of sensors so as to maximize what is known about the set of system variables, as a whole, under both Gaussian or non-Gaussian sensor measurement distribution assumptions.

The following sections detail the procedure for obtaining the Fisher information value for a given network of sensors. In summary, the ASPEN Plus software environment is used to simulate the nonlinear IGCC process over a range of operating points. Then, a probability distribution for each intermediate and output process variable is constructed, given the probability distributions resulting from sensors placed on input variables using kernel density estimation. A reweighting scheme is posed to generate the intermediate and output distributions due to the placement of various sensors networks and measurement accuracies due to different types of sensors. Lastly, a nonlinear, stochastic (binary) integer problem is formulated to maximize a normalized Fisher information metric resulting from the entire network of on-line sensors.

3. Computation of Fisher information

For a sequence of n observations of the random variable X, Fisher information may be calculated via order statistics; however, this route is shown to be quite complicated due to performing n levels of integration. Park [50] presents a decomposition approach to simplifying this calculation to performing a double integral. Although this type of approach is useful for obtaining the Fisher information when given a set of observations, this paper computes an approximation of the Fisher information by constructing the distribution using kernel density estimation.

Using the ASPEN Plus environment, a comprehensive model of the IGCC process is used to simulate the steady-state performance of the ASU, gasifier, and power generation operations. This nonlinear ASPEN model is used to estimate the set of unmeasured variables using the data acquired from the process variables directly measured through the network of sensors physically deployed within the plant. Internal operating conditions in the process can be analyzed by varying a set of S^{in} input variables, including coal and oxygen flow rate. These input variable operating conditions uniformly span a sample space surrounding their nominal values. A set of N_s input variable operating conditions are generated using Hammersley sequencing, a low-discrepancy sampling method, to generate the uniform sample space. This sampling method is chosen over common Monte-Carlo sampling techniques to provide a more uniform distribution across an d-dimensional sample space, where the number of sample points necessary to sufficiently cover an d-dimensional space can be significantly reduced by using the Hammersley sampling technique [51,52]. Then, the IGCC process is simulated N_s times, once per input operating condition, to generate a corresponding vector of points for S^{out} intermediate and output process variables, including the syngas temperature, pressure, and mass flow rate, among others. The resulting vector set of intermediate and output variables can be used to capture the nonlinear effects of the IGCC process, as well as the variability of downstream variables resulting from a uniformly distributed set of input variable sample points. The IGCC process is simulated across a space of operating points to generate the probability distribution of each intermediate and output variable due to variations in the input variables and the nonlinear process behavior. From this, the information about each of the process variables can be obtained as a result of a shift in the true steady-state operating point.

The following section outlines the reweighting approach used to compute the Fisher information about each process variable due to the placement of sensors in the network, and hence, altering the underlying distributions of the process variables.

3.1. Reweighting approach

The reweighting approach used in this paper is of that proposed by [53], called Better Optimization for Nonlinear Uncertain Systems (BONUS). The purpose of this algorithm is to compare samples taken from a uniformly distributed sample space to a new reference distribution, in order to create a set of distribution weights which can be used to reweight the output distribution function. This reweighting approach is beneficial for eliminating the need to recreate a set of new sample points through simulation of the process behavior. Thus, the ASPEN simulation model only needs to compute the IGCC process behavior for the set of uniform sample points, and not for each combination of potential on-line sensor networks, thereby significantly reducing the overall computational time. This approach has been extensively tested for various models including power plant system models like the one used in this paper [53,54].

Fig. 2 illustrates the nature of this reweighing scheme. On the first iteration, a set of N_s sample points uniformly distributed across a d-dimensional sample space are used to perform N_s simulation replications of the IGCC process (i.e., at various operating points). Let $f_0(x_i)$ be the probability density function (pdf) associated with the base input distribution for the input variable x_i, $i = 1, 2, \ldots, S^{in}$, respectively. Following the simulation of the IGCC process at iteration $t = 0$, let $F_0(y_j)$ be the base cumulative distribution function (cdf) associated with the intermediate and output variable $y_j, j = 1, 2, \ldots, S^{out}$, respectively, where $y_j = h(x_1, x_2, \ldots, x_{S^{in}})$ is the nonlinear

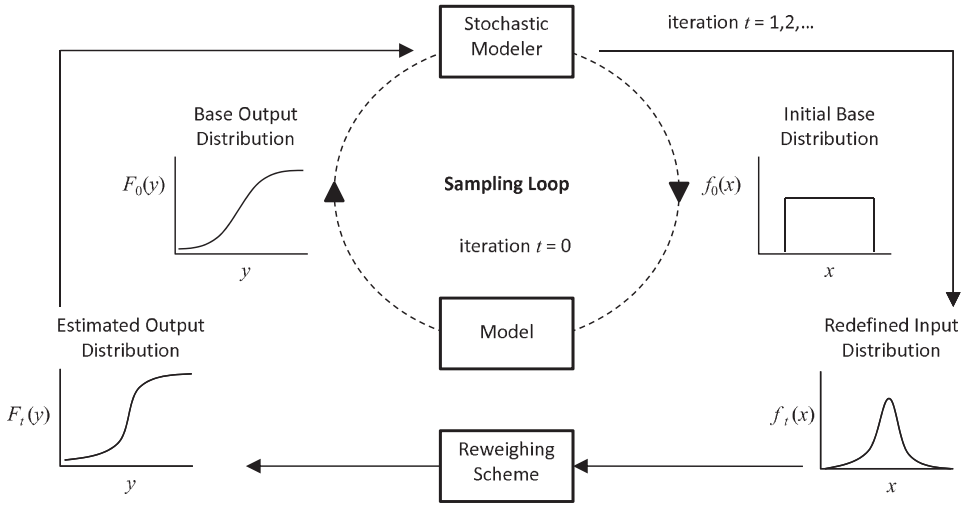

Fig. 2. The reweighting approach.

transformation from each input variable, x_i, to the downstream variable y_j.

Next, consider when a new input distribution is defined, such as when a sensor is placed at the location of this input variable. The redefined distribution, $f_t(x_i)$, at iteration t is used to create a set of weights

$$W_t(x_i) = f_t(x_i)/f_0(x_i), \quad i = 1,2,\ldots,S^{in}, \tag{2}$$

which gives the likelihood ratio between the redefined and base distributions. Given that the input variables act independently, these weights are used to construct the resulting distribution for the downstream intermediate and output variables at iteration t by multiplying the associated weights $W_t(x_i)$ with the base distribution $f_0(y_j)$,

$$f_t(y_j) = f_0(y_j)\prod_{i=1}^{S^{in}}(1+\gamma_{i,j}(W_t(x_i)-1)), \quad j = 1,2,\ldots,S^{out}, \tag{3}$$

where $\gamma_{i,j} = 1(0)$ if variable y_j is (is not) downstream of x_i. The distribution $f_t(y_j)$ in (3) is then normalized using

$$\hat{f}_t(y_j) = \frac{f_t(y_j)}{\sum_{n=1}^{N_s} f_t(y_j(n))(y_j(n+1)-y_j(n-1))/2}. \tag{4}$$

This reweighting approach can also be used when a sensor is placed at the location of an intermediate process variable, to construct the resulting change in distributions of corresponding downstream variables. By eliminating the need to regenerate a new set of N_s sample points through simulation of the IGCC process at each iteration t, the BONUS reweighting algorithm provides an efficient method for calculating the Fisher information and level of observation order resulting from several reconfigurations of a network of on-line sensors. Moreover, various underlying distributions corresponding to sensor accuracies can be readily analyzed, without increasing the computational burden. This approach can also be used for unmeasured disturbances due to changes in coal quality, for example.

3.2. Fisher information from kernel density estimation

A probability density function for the intermediate and output process variables is approximated through the kernel density technique, given by

$$p(y_n) = \sum_{m=1}^{N_s}\frac{1}{\sqrt{2\pi}}\exp(-((y_n-y_m)/h)^2), \tag{5}$$

at each sample point, y_n,$n = 1, 2, \ldots, N_s$. A window of $h = 1.06\sigma/N_s^{1/5}$ is defined, where σ^2 is the variance of the set of samples $\{y_1, y_2, \ldots, y_{N_s}\}$. Assume that the shift-invariant property holds for a small $\epsilon \geqslant 0$ change in the parameter θ_y (i.e., the mean value). This is a viable assumption around the mean operating conditions in a IGCC process, since it is desirable to operate the plant within a chemically stable region. Kernel density functions $p(y_n + \epsilon)$ and $p(y_n - \epsilon)$ are then computed from (5), and used to generate an approximation to the first order derivative, $\partial\, p(y_n)/\partial\theta_y$, given by

$$\partial p(y_n)/\partial\theta_y \approx (p(y_n+\epsilon) - p(y_n-\epsilon))/2\epsilon. \tag{6}$$

The Fisher information is then obtained by substituting (6) into the discrete approximation of (1) to yield

$$I_Y(\theta_y) = \sum_{n=1}^{N_s}(y_n - y_{n-1})(\partial p(y_n)/\partial\theta_y)^2/p(y_n), \tag{7}$$

which constructs a series of right-hand rectangles at $(\partial p(y_n)/\partial\theta_y)^2/p(y_n)$ to approximate the integral function in the expectation.

The objective of the sensor placement problem is to maximize the amount of information about the IGCC process from a network of sensors. The following section applies Fisher information as a metric of observation order within an optimization problem for placing sensors in various locations throughout the IGCC plant, subject to sensor cost constraints.

4. Optimization problem

In the sensor placement problem, the objective is to determine the optimal location of a network of sensors, such that when combined with a comprehensive system model, the variability of the unmeasured process variable estimations can be minimized. Within the scope of this paper, Fisher information is viewed as a statistical measure of system order, and hence, the objective is defined to maximize some function of the Fisher information over all feasible networks of sensors, subject to budget constraints.

To accomplish this goal, an optimization problem is formulated as a nonlinear, stochastic (binary) integer program, where the objective is to maximize the overall Fisher information, subject to the costs associated with placing a network of on-line sensors

$$\max_{w_j \in \mathbb{W}} \sum_{j=1}^{S^{out}} f_j(\mathbf{w}, \mathbf{Y}) w_j, \tag{8}$$

$$\text{s.t.} \sum_{j=1}^{S^{out}} C_j w_j \leqslant B, \tag{9}$$

$$w_j \in \{0,1\}, \quad j = 1,2,\ldots,S^{out}, \tag{10}$$

where C_j is the cost associated with the purchase, deployment, and maintenance of sensor j, and B is the total sensor budget. The binary variable $w_j = 1(0)$ represents the decision to place (not place) sensor j in the network of on-line sensors, where $\mathbb{W}$ constitutes the set of all feasible sensor networks. The objective term, $f_j(\mathbf{w},\mathbf{Y})$, is defined as a function of the Fisher information that results from the network of sensors, $\mathbf{w} = \{w_j \in \{0,1\}, j = 1, 2, \ldots, S^{out}\}$, and the random variables $\mathbf{Y} = \{Y_j, j = 1, 2, \ldots, S^{out}\}$ associated with the measurement uncertainties in the intermediate and output process variables.

The objective term, $f_j(\mathbf{w},\mathbf{Y})$, is designed in the following way. Assume that the information related to a process variable is always greater if a sensor is placed on-line at that specific location. Otherwise, the information gained from estimating the variable would supersede that gained from the accuracy of the sensor measuring the variable directly, and hence, a sensor provides no additional information at that location. Let $I^s_{Y_j}(\theta_{y_j}|w_k = 1)$ represent the Fisher information of θ_{y_j} resulting from a sensor placed at location $k = 1, 2, \ldots, S^{out}$, and let $I^{ns}_{Y_j}(\theta_{y_j}) \equiv I^{ns}_{Y_j}(\theta_{y_j}|w_k = 0)$, $k = 1, 2, \ldots, S^{out}$ represent the Fisher information of θ_{y_j} resulting from no sensors placed in the network of intermediate and output variables, such that $I^s_{Y_j}(\theta_{y_j}|w_k = 1) \geqslant I^{ns}_{Y_j}(\theta_{y_j}), j = 1,2,\ldots,S^{out}$. One candidate function for $f_j(\mathbf{w},\mathbf{Y})$ can be defined as

$$f_j^A(\mathbf{w},\mathbf{Y}) = 1 - I^{ns}_{Y_j}(\theta_{y_j})/I^s_{Y_j}(\theta_{y_j}|w_j = 1), \tag{11}$$

where $0 \leqslant f_j^A(\mathbf{w},\mathbf{Y}) \leqslant 1$. Values of $f_j^A(\mathbf{w},\mathbf{Y})$ close to zero (one) correspond to the smallest (largest) change in information gained from placing a sensor at location j. By normalizing the Fisher information for each process variable between zero and one, it is possible to optimize the placement of sensors across several variable attributes, such as mass-flow, temperature, and pressure, for example, by using a Pareto analysis to determine the set of sensors that provide the largest gain for estimating the state of the dynamical system.

Eq. (11), however, does not capture the effects of placing a sensor in the network upstream of location j. Suppose a sensor is placed at location k, and variable j is downstream of (i.e., dependent on) variable k. The information gained from placing the sensor at location k can also increase the amount of information about the variable at location j. A second candidate function for $f_j(\mathbf{w},\mathbf{Y})$ can be defined as

$$f_j^B(\mathbf{w},\mathbf{Y}) = \sum_{k=1}^{S^{out}} \left(1 - I^{ns}_{Y_j}(\theta_{y_j})/I^s_{Y_j}(\theta_{y_j}|w_k = 1)\right), \tag{12}$$

which captures the overall effect that placing a sensor has on all other process variables by summing the resulting information gain from placing a sensor at location k across the entire set of intermediate and output process variables. The Fisher information $I^s_{Y_j}(\theta_{y_j}|w_k = 1) = I^{ns}_{Y_j}(\theta_{y_j})$ if variable j is not downstream of variable k. Otherwise, $I^s_{Y_j}(\theta_{y_j}|w_k = 1)$ can be computed using the reweighting scheme outlined in Section 2.

The following section provides a computational analysis of the use of Fisher information in determining the optimal location of on-line sensors in the IGCC process.

5. Computational results

This section illustrates a case study of the IGCC power plant, where a set of sensors measuring $S^{in} = 8$ input process variables, $x_1, x_2, \ldots, x_8$, are used to determine the placement of sensors across a set of $S^{out} = 24$ intermediate and output variables, $y_1, y_2, \ldots, y_{24}$. Tables 1 and 2 list the input variables and intermediate and output variables under consideration, respectively, along with the nominal operating conditions. A set of $N_s = 800$ operating conditions was generated across a uniform 8-dimensional sample space, corresponding to a set of eight input variables varied ±10% of their nominal conditions using the Hammersley sequence sampling method. Then, for each set of operating conditions, the corresponding intermediate and output variable conditions are generated using a steady-state model developed in the ASPEN Plus simulation environment. A distribution function is constructed from these sets of sample points using the kernel density technique in (5), which serves as the base distribution in the BONUS reweighting scheme outlined in Section 3.1.

Suppose the input sensors measurement errors are normally distributed, with mean value given in Table 1, and variance defined by six standard deviations spanning ±10% of the nominal value. Note that the use of Fisher information is not restricted to Gaussian distributions, and other underlying distributions for the set of sensors can be analyzed, such as uniform, triangular, or trapezoidal distributions. Discrete distributions can be addressed through suitable continuous approximations to comply with the Fisher information partial differentiation term. Fig. 3 illustrates the stream paths from the input to output process variables [11,55]. The distribution function for $Y_j, j = 1, 2, \ldots, 24$ is constructed using BONUS by reweighting the base distribution of Y_j obtained from the ASPEN simulations by the ratio of the sensor distribution of X_i, $i = 1, 2, \ldots, 8$ to the base distribution of X_i, provided that Y_j is downstream of each X_i. The resultant distribution at each Y_j corresponds to the variability of estimating Y_j if no sensors are placed across the set of intermediate and output variable locations. From this distribution, the quantity $I^{ns}_{Y_j}(\theta_{y_j})$ is obtained as outlined in Section 3.1.

To verify the validity of the reweighting approach, the ASPEN model was first simulated using the above uniform distribution across each of the input variables. Then, the model was simulated using the normal distributions at each of the input variables with standard deviation according to Table 1. No significant difference in the calculation of the Fisher information resulted for the input, intermediate, and output variables between the two simulation approaches. This occurred primarily because (a) there were sufficient number of sample points taken ($N_s = 800$), (b) the Hammersley sampling technique covers the 8-dimensional sample space uniformly, and (c) the reweighting approach only undergoes one iteration when computing the Fisher information for a given set of input variable distributions. The reweighting approach is a useful technique when comparing sensors with contrasting variability, as opposed to rerunning the time-consuming simulation.

Table 1
Input process variables.

x_i	Description	Nominal	Units
1	Oxygen flow rate entering ASU	157,392	kg/h
2	Coal slurry flow rate	192,922	kg/h
3	Air flow rate to gas turbine compressor	2,962,683	kg/h
4	Recycled HRSG steam temperature	414	K
5	Recycled HRSG steam pressure	526	KPa
6	Recycled HRSG water temperature	369	K
7	Gasifier temperature	1644	K
8	Gasifier pressure	2806	KPa

Table 2
Intermediate and output process variables.

y_j	Description	Stream[a]	Nominal	Units
1	Gasifier syngas flow rate	RXROUT	393,475	kg/h
2	Syngas CO flow rate	RXROUT	224,637	kg/h
3	Syngas CO_2 flow rate	RXROUT	88,051	kg/h
4	Syngas temperature	RXROUT	1644	K
5	Syngas pressure	RXROUT	2806	KPa
6	Low pressure steam turbine temp.	TORECIR	369	K
7	Gas turbine combustor burn temp.	POC2	1628	K
8	Gas turbine combustor exit temp.	POC3	1533	K
9	Gas turbine high pressure exhaust stream temp.	GTPC3	621	K
10	Gas turbine low pressure exhaust stream temp.	GTPC9	404	K
11	Gas turbine expander output temp.	GTPOC	872	K
12	Fluegas flow rate exiting gas turbine expander	6X	5,760,623	kg/h
13	Syngas flow rate after solids removal	RAWGAS	467,200	kg/h
14	Coal slurry flow rate entering gasifier	COALD	21,170	kg/h
15	Oxygen flow rate into gasifier	O2GAS	157,452	kg/h
16	Oxygen flow rate exiting ASU	GASIFOXY	157,452	kg/h
17	Acidgas flow rate	FUEL1	344,996	kg/h
18	Gas turbine compressor leakage flow rate	XCLEAK	2052	kg/h
19	Flow rate into high pressure steam turbine	TOHPTUR	621,421	kg/h
20	Coal slurry feed flow rate	COALFEED	192,922	kg/h
21	Slag extracted from syngas	SLAG	15,805	kg/h
22	Fines extracted from syngas	FINES	5363	kg/h
23	Gasifier heat output	QGASIF	2.47e7	Btu/h
24	Recycled HRSG steam heat output	QRDEA	3.27e8	Btu/h

[a] Stream notation refers to DOE/NETL model [11].

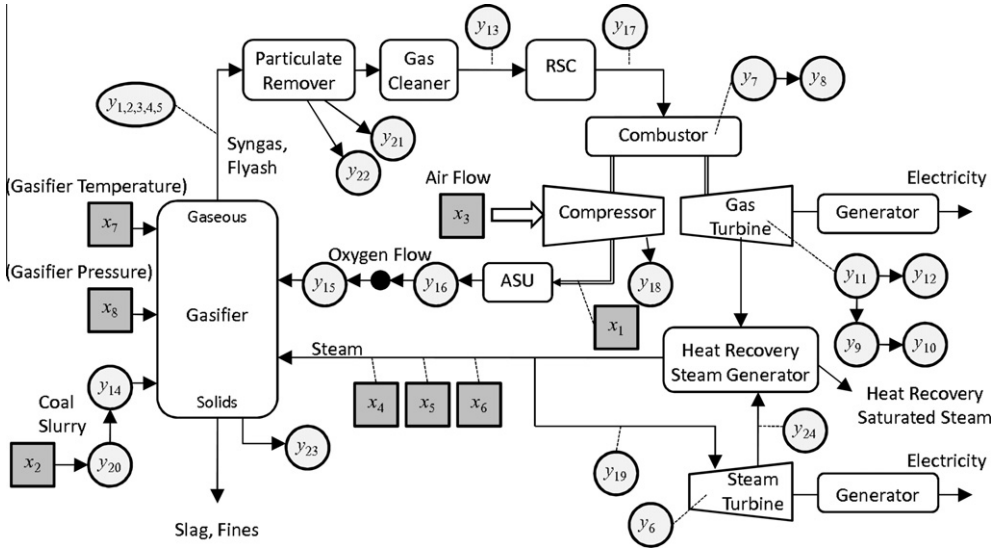

Fig. 3. IGCC process variable flowchart.

For each intermediate and output process variable, three types of sensors are considered with accuracies (six standard deviations) of ±5%, ±2.5%, and ±1%. Table 3 lists generic costs associated with the purchase, operation, and maintenance of each type of sensor. Both the cost and accuracies of the sensors are arbitrary, and may be substituted with values found in practice when available. The Fisher information $I^s_{Y_j}(\theta_{y_j}|w_k=1)$ given a type of sensor is placed at location k is obtained by determining if variable j is downstream of variable k (i.e., $\gamma_{i,j}\in\{0,1\}$). If so, then the distribution of Y_j is obtained using the BONUS reweighting scheme.

Let the binary variable $w_{j,\tau}=1(0)$ correspond to the decision to place a sensor of type $\tau=1$, 2, 3 (low, medium, high accuracy, respectively) at location j. The optimization problem in (8)–(10) is modified to include the consideration of multiple sensor types as follows:

$$\max_{w_{j,\tau}\in\mathbb{W}} \sum_{\tau=1}^{3}\sum_{j=1}^{24} f_{j,\tau}(\mathbf{w},\mathbf{Y})w_{j,\tau} \tag{13}$$

$$\text{s.t.} \sum_{\tau=1}^{3}\sum_{j=1}^{24} C_{j,\tau}w_{j,\tau} \leqslant B, \tag{14}$$

$$\sum_{\tau=1}^{3} w_{j,\tau} \leqslant 1, \quad j=1,2,\ldots,24 \tag{15}$$

$$w_{j,\tau}\in\{0,1\}, \quad j=1,2,\ldots,24, \quad \tau=1,2,3 \tag{16}$$

where the objective, $f_{j,\tau}(\mathbf{w},\mathbf{Y})$, is a function of the Fisher information when a sensor of type τ is placed at location j. Constraint (15) restricts the use of only one type of sensor at each location. Note that constraints may also be incorporated at each individual sensor location that limits the minimum allowable Fisher information value at

Table 3
Intermediate and output sensor costs.

y_j	Low accuracy	Medium accuracy	High accuracy
1	$80,000	$160,000	$300,000
2	$80,000	$160,000	$300,000
3	$80,000	$160,000	$300,000
4	$400,000	$800,000	$1,200,000
5	$200,000	$350,000	$500,000
6	$50,000	$100,000	$200,000
7	$400,000	$800,000	$1,200,000
8	$400,000	$800,000	$1,200,000
9	$50,000	$100,000	$200,000
10	$50,000	$100,000	$200,000
11	$100,000	$200,000	$300,000
12	$120,000	$300,000	$450,000
13	$120,000	$300,000	$450,000
14	$80,000	$160,000	$300,000
15	$80,000	$160,000	$300,000
16	$80,000	$160,000	$300,000
17	$80,000	$160,000	$300,000
18	$80,000	$160,000	$300,000
19	$120,000	$300,000	$450,000
20	$80,000	$160,000	$300,000
21	$80,000	$160,000	$300,000
22	$80,000	$160,000	$300,000
23	$120,000	$300,000	$450,000
24	$120,000	$300,000	$450,000

Table 4
Computed objective values, f_j^B, for each sensor type.

Sensor j	Low accuracy	Medium accuracy	High accuracy
1	0.9100	8.6612	10.6078
2	9.8488	10.7561	10.9649
3	10.5601	10.8862	10.9898
4	7.8290	10.1407	10.8627
5	7.8989	10.1472	10.8613
6	0.1036	0.7760	0.9643
7	4.6106	5.6794	5.9470
8	3.7799	4.7002	4.9529
9	1.9262	1.9832	1.9981
10	0.9940	0.9989	1.0002
11	2.5901	2.9110	2.9845
12	0.0002	0.7054	0.9531
13	0.9188	6.2690	7.6865
14	12.4675	15.8420	16.8025
15	12.4553	15.8393	16.8083
16	13.3944	16.8241	17.8059
17	3.6553	6.2014	6.8691
18	0.9389	0.9849	0.9978
19	0.0002	0.0002	0.0002
20	13.4061	16.8267	17.8000
21	0.7492	0.9375	0.9902
22	0.7492	0.9375	0.9902
23	1.0002	1.0002	1.0002
24	0.0002	0.0002	0.0002

that location (i.e., maximum measurement error). However, by doing so may lead to cases where no solution can be obtained. Instead, the resulting network placement and Fisher information values can be analyzed to determine if the solution is indeed acceptable.

Table 4 lists the computed objective values using the normalized function $f_j^B(\mathbf{w},\mathbf{Y})$ from (12). As the sensor accuracy increases, the value of f_j^B increases at each location due to the decrease in measurement variability, resulting in an increase in information pertaining to the variable's true value. Note that some variables, such as the syngas flow rate (y_1) and the oxygen flow rate exiting the gas turbine expander (y_{12}), exhibit large increases of information by increasing the sensor accuracy at these locations. Other variables, such as the gas turbine low pressure exhaust stream temperature (y_{10}) and the flow rate into the high pressure steam turbine (y_{19}, do not significantly benefit from the increase in accuracy.

Table 5
Measurement variation of the IGCC power production and gasifier performance using the optimal sensor network versus no sensors deployed.

	Nominal	Standard deviation optimal (no sensors)	Units
IGCC power production			
Gas turbine power production	424.94	2.26 (43.11)	MWE
Steam turbine power production	251.97	0.71 (0.71)	MWE
Miscellaneous power production	−67.41	0.25 (4.62)	MWE
Auxiliary power production	18.29	1.35 (1.35)	MWE
Total plant power production	591.22	2.16 (43.73)	MWE
Gasifier performance			
Oxygen flow rate	157,452	655 (13,386)	kg/h
Coal flow rate	192,922	803 (10,874)	kg/h
Slag flow rate	15,805	46 (1,097)	kg/h
Fines flow rate	5363	16 (372)	kg/h
Syngas temperature	1645	370 (370)	K
Syngas pressure	2806	23 (234)	KPa

Table 6
Optimal sensor locations and sensor types due to budget constraints, B (where $w_{j,\tau} = 1$).

$500,000	$1,000,000	$1,500,000	$2,000,000	$2,500,000
$w_{2,1}$	$w_{2,1}$, $w_{1,2}$	$w_{2,1}$, $w_{1,2}$	$w_{2,1}$, $w_{1,2}$	$w_{2,1}$, $w_{1,2}$
$w_{3,1}$	$w_{3,1}$, $w_{16,2}$	$w_{3,1}$, $w_{14,2}$	$w_{3,1}$, $w_{14,2}$	$w_{3,1}$, $w_{5,2}$
$w_{14,1}$	$w_{5,1}$	$w_{5,1}$, $w_{15,2}$	$w_{4,1}$, $w_{15,2}$	$w_{4,1}$, $w_{13,2}$
$w_{15,1}$	$w_{14,1}$	$w_{9,1}$, $w_{16,2}$	$w_{5,1}$, $w_{16,2}$	$w_{6,1}$, $w_{14,2}$
$w_{16,1}$	$w_{15,1}$	$w_{11,1}$, $w_{17,2}$	$w_{9,1}$, $w_{17,2}$	$w_{9,1}$, $w_{15,2}$
$w_{20,1}$	$w_{17,1}$	$w_{20,2}$	$w_{10,1}$, $w_{20,2}$	$w_{10,1}$, $w_{16,2}$
	$w_{20,1}$		$w_{11,1}$	$w_{11,1}$, $w_{17,2}$
			$w_{18,1}$	$w_{18,1}$, $w_{20,2}$

Consider the case when the total budget is B = $1,500,000. The solution to the optimization problem in (13)–(16) places a network of low accuracy sensors at locations y_2, y_3, y_5, y_9 and y_{11}, and medium accuracy sensors at locations y_1, y_{14}, y_{15}, y_{16}, y_{17} and y_{20}. The resulting standard deviation in the IGCC plant power production and gasifier performance are provided in Table 5, in comparison with the standard deviation resulting from the baseline case when no sensors are deployed across the intermediate and output process variable locations. At these conditions, the plant thermal efficiency is 40.65%, with a standard deviation of 0.07%. To illustrate the effect of the budget on the placement of sensors, Table 6 lists the location and type of sensor placed in the network as a function of the total budget, ranging from B = $500,000 to B = $2,500,000. As the budget increases, the number of sensors placed within the network increases, as does the accuracy of the sensors selected. Fig. 4 shows the standard deviation of the coal and oxygen flow rates into the gasifier, and the gasifier temperature and pressure as a function of the total budget. The stair step effect is a result of the type of sensor used to measure those process variables. Note that the placement of a low accuracy sensor to directly measure the syngas pressure significantly improves the information about the true pressure value, as opposed to inferring this quantity using a virtual sensor. However, increasing the accuracy of this pressure sensor yields only a slight improvement to the measurement variance.

6. Extension to dynamic systems

This paper addresses the sensor placement problem by analyzing the steady-state behavior of the IGCC process. A natural

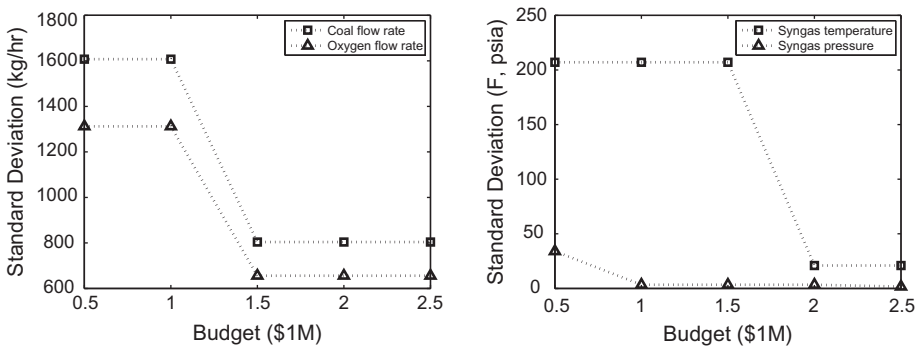

Fig. 4. Gasifier performance accuracy resulting from the placement of different sensor types.

extension is to capture the transient behavior of the process through a dynamic model, where uncertainties can be prevalent in both the system and measurement dynamics. A well-developed sequential algorithm for estimating the variability of the state variables for a linear system is the Kalman Filter (KF), an optimal mathematical recursion that computes the covariance of the process variables from the system dynamics, given a zero-mean Gaussian distribution of the system and measurement noise [56]. Systems that involve nonlinear dynamics can be addressed using the Extended Kalman Filter (EKF), a suboptimal variation of the KF that utilizes a first order linearization of the system equations around the nominal operating point. Here, the system noise and measurement noise are assumed to be zero-mean, Gaussian white noise. The objective is to sequentially update the estimation of the unknown process variables using the set of $t = 1, 2, \ldots$ acquired measurements, characterized by a Gaussian distribution with mean μ_t and covariance P_t at each discrete time t. Note that the dual to the KF, called the information filter, yields a sequential estimate of the inverse of the process variable covariance. Since this operates on a linear, Gaussian system (i.e., an efficient estimator), the Cramer–Rao equality holds and the information filter yields a sequential value of the Fisher information.

To relax the Gaussian assumption on the system and measurement noise, a particle filter can be applied to sequentially estimate the distribution of each unmeasured process variable. For the sensor placement problem, generating the estimated value is not essential, but the variable distribution function generated by the particle filter can be used in the sequential calculation of the Fisher information in (7). Therefore, Fisher information can be used to analyze the transient behavior of a IGCC process governed by nonlinear dynamics and for non-Gaussian system and measurement noise. Future extensions of the use of Fisher information for the dynamic process of the IGCC power plant can be explored to investigate its impact on the sensor placement problem.

7. Conclusions

Fisher information is a statistical measure that can be used to capture the amount of order in a system, by taking the expectation of the amount of change in the distribution of a random variable with respect to the change in a parameter contained within the distribution. This local measure of system order can also be used to indicate the level of observation order for an unknown parameter value, which is shown to have direct implications to optimal sensor placement problems. In advanced power systems, the sensor placement problem corresponds to finding the optimal number, location, and type of sensors to place across a network of measurable process variables. Considering cost limitations, Fisher information can be used within a stochastic optimization problem to determine the locations where sensors should be physically placed (i.e., measured process variables) and those which can be observed (i.e., unmeasured process variables).

This paper presents a method to approximate the Fisher information about the mean value of a process variable using a combination of kernel density estimation and a reweighting scheme called BONUS. The optimization problem is formulated as a nonlinear, stochastic (binary) integer program, where the objective is to maximize the overall (normalized) Fisher information gained from deploying a network of on-line sensors, subject to a given budget constraint. Sensors with various levels of accuracy are considered, and the type and placement of each sensor is determined by solving the optimization problem. Results are presented that compare the effects of budget constraints on the deployment of sensors. The key advantage to using this approach to solving the sensor placement problem is that the use of Fisher information as a measure of observation order generalizes the Gaussian assumption on system and measurement noise, and is applicable to systems governed by nonlinear behavior. Future research can extend or compare the use of Fisher information to sensor placement problems that require fault detection or specify reliability constraints.

References

[1] Ali Y, Narasimhan S. Sensor network design for maximizing reliability of linear processes. AIChE J 1993;39(5):820–8.
[2] Alonso AA, Kevrekidis IG, Banga JR, Frouzakis CE. Optimal sensor location and reduced order observer design for distributed process systems. Comput Chem Eng 2004;28:27–35.
[3] Chmielewski DJ, Palmer T, Manousiouthakis V. On the theory of optimal sensor placement. AIChE J 2002;48(5):1001–12.
[4] Bagajewicz M, Fuxman A, Uribe A. Instrumentation network design and upgrade for process monitoring and fault detection. Am Inst Chem Eng J 2004;50(8):1870–80.
[5] Bhushan M, Narasimhan S, Rengaswamy R. Robust sensor network design for fault diagnosis. Comput Chem Eng 2008;32:1067–84.
[6] Li F, Upadhyaya BR. Design of sensor placement for an integral pressurized water reactor using fault diagnostic observability and reliability criteria. Nucl Technol 2011;173(1):17–25.
[7] He F, Li Z, Liu P, Maa L, Pistikopoulos EN. Operation window and part-load performance study of a syngas fired gas turbine. Appl Energy 2012;89:133–41.
[8] Park SK, Ahn J, Kim TS. Performance evaluation of integrated gasification solid oxide fuel cell/gas turbine systems including carbon dioxide capture. Appl Energy 2011;88:2976–87.
[9] Pérez-Fortes M, Bojarski AD, Puigjaner L. Advanced simulation environment for clean power production in IGCC plants. Comput Chem Eng 2011;35:1501–20.
[10] Tampa electric polk power station integrated gasification combined cycle report. Final technical report, August 2002. <http://www.tampaelectric.com/data/files/PolkDOEFinalTechnicalReport.pdf>.
[11] US Department of Energy National Energy Technology Laboratory. EPA study – case 8: IGCC. Technical report DOE/NETL-401/042606, November 2006. Available upon request from the USDOE.
[12] Martelli E, Kreutz T, Carbo M, Consonni S, Jansen D. Shell coal IGCCS with carbon capture: conventional gas quench vs. innovative configurations. Appl Energy 2011;88:3978–89.
[13] Giuffrida A, Romano MC, Lozza GG. Thermodynamic assessment of IGCC power plants with hot fuel gas desulfurization. Appl Energy 2010;87:3374–83.
[14] Giuffrida A, Romano MC, Lozza G. Thermodynamic analysis of air-blown gasification for IGCC applications. Appl Energy 2011;88:3949–58.

[15] Kim YS, Lee JJ, Kim TS, Sohn JL, Joo YJ. Performance analysis of a syngas-fed gas turbine considering the operating limitations of its components. Appl Energy 2010;87:1602–11.
[16] Lee JJ, Kim YS, Cha KS, Kim TS, Sohn JL, Joo YJ. Influence of system integration options on the performance of an integrated gasification combined cycle power plant. Appl Energy 2009;86:1788–96.
[17] Deng K, Wu J, Wang Z, Lee B, Guida R. On-line compositional analysis in coal gasification environment using laser-induced plasma technology. Proc SPIE 2006;6314. 631410-(1-8).
[18] Wu J, Deng K, Guida R, Lee B. Fiber-optic photo-acoustic spectroscopy sensor for harsh environment gas detection. Proc SPIE 2007;6698. 66980E-(1-7).
[19] Colantuoni G, Padmanabhan L. Optimal sensor location for tubular-flow reactor systems. Chem Eng Sci 1977;32(9):1035–49.
[20] Harris TJ, Macgregor JF, Wright JD. Optimal sensor location with an application to a packed bed tubular reactor. AIChE J 1980;26(6):910–6.
[21] Jorgensen SB, Goldschmidt L, Clement K. A sensor location procedure for chemical processes. Comput Chem Eng 1984;8(3–4):195–204.
[22] Kumar S, Seinfeld SH. Optimal location of measurements in tubular reactors. Chem Eng Sci 1978;33(11):1507–16.
[23] Omatu S, Koide S, Soeda T. Optimal sensor location for a linear distributed parameter system. IEEE Trans Autom Control 1978;23(4):665–73.
[24] Romagnoli J, Alvarez J, Stephanopolus G. Variable measurement structures for process control. Int J Control 1981;33(2):269–89.
[25] Singh A, Han J. Determining optimal sensor locations for state and parameter estimation for stable nonlinear systems. Ind Eng Chem Res 2005;44(15): 5645–59.
[26] Chang CT, Mah KN, Tsai CS. A simple design strategy for fault monitoring systems. AICHE J 1993;39(7):1146–63.
[27] Kelly JD, Zyngier D. A new and improved MILP formulation to optimize observability, redundancy and precision for sensor network problems. AIChE J 2008;54(5):1282–91.
[28] Madron F, Veverka V. Optimal selection of measuring points in complex plants by linear models. AIChE J 1992;38(2):227–36.
[29] Ragot J, Maquin D. Fault measurement detection in an urban water supply network. J Process Cont 2006;16(9):887–902.
[30] Bagajewicz MJ. Design and retrofit of sensor networks in process plants. AIChE J 1997;43:2300–6.
[31] Muske KR, Georgakis C. Optimal measurement system design for chemical processes. AIChE J 2003;49(6):1488–94.
[32] Isidori A. Nonlinear control systems. 3rd ed. New York: Springer-Verlag; 1995.
[33] Hermann R, Kerner AJ. Nonlinear controllability and observability. IEEE Trans Autom Control 1977;22(5):728–40.
[34] Lopez T, Alvarez J. On the effect of the estimation structure in the functioning of a nonlinear copolymer reactor estimator. J Process Control 2004;14(1):99–109.
[35] Wouwer AV, Point N, Porteman S, Remy M. An approach to the selection of optimal sensor locations in distributed parameter systems. J Process Control 2000;10(4):291–300.
[36] Qureshi ZH, Ng TS, Goodwin GC. Optimum experimental design for identification of distributed systems. Int J Control 1980;31(1):21–9.
[37] Basseville M, Benveniste A, Moustakides G, Rougee A. Optimal sensor location for detecting changes in dynamical behavior. IEEE Trans Autom Control 1987;32(12):1067–75.
[38] Fisher RA. On the mathematical foundation of theoretical statistics. Philos Trans Roy Soc Lond 1922;222:309–68.
[39] Masi M. Generalized information-entropy measures and Fisher information. NASA Astrophys Data Syst 2008;1–16. <http://arxiv.org/abs/cond-mat/0611300v2>.
[40] Frieden BR, Gatenby RA. Exploratory data analysis using fisher information. London: Springer-Verlag; 2007.
[41] Jauffret C. Observability and Fisher information matrix in nonlinear regression. IEEE Trans Aerospace Elect Syst 2007;43(2):756–9.
[42] Fath BD, Cabezas H. Exergy and Fisher information as ecological indices. Ecol Modell 2004;174:25–35.
[43] Karunanithi AT, Cabezas H, Frieden BR, Pawlowski CW. Detection and assessment of ecosystem regime shifts from Fisher information. Ecol Soc 2008;13(1) [Article 22].
[44] Pawlowski CW, Fath BD, Mayer AL, Cabezas H. Towards a sustainability index using information theory. Energy 2005;30:1221–31.
[45] Shastri Y, Diwekar UM. Sustainable ecosystem management using optimal control theory: Part 1 (deterministic systems). J Theor Biol 2006;241:506–21.
[46] Hawkins RJ, Frieden BR. Fisher information and equilibrium distributions in econophysics. Phys Lett A 2004;322:126–30.
[47] Nguyen DT, Bagajewicz MJ. On the impact of sensor maintenance policies on stochastic-based accuracy. Comput Chem Eng 2009;33:1491–8.
[48] Nguyen DT, Sugumar SK, Bagajewicz MJ. Software accuracy-based sensor network design and upgrade in process plants. Ind Eng Chem Res 2011;50:4850–7.
[49] Schladt M, Hu B. Soft sensors based on nonlinear steady-state data reconciliation in the process industry. Chem Eng Proc 2007;46:1107–15.
[50] Park S. Fisher information in order statistics. J Am Stat Assoc 1996;91(433):385–90.
[51] Diwekar UM, Kalagnanam JR. Efficient sampling technique for optimization under uncertainty. AIChE J 1997;43:440–7.
[52] Diwekar UM. A novel sampling approach to combinatorial optimization under uncertainty. Comput Opt Appl 2003;24:335–71.
[53] Sahin K, Diwekar UM. Better optimization for nonlinear uncertain systems (BONUS): a new algorithm for stochastic programming using reweighting through kernel density estimation. Ann Oper Res 2004;132:47–68.
[54] Salazar J, Diwekar UM, Zitney S. Minimization of water consumption under uncertainty for a pulverized coal power plant. Environ Sci Technol 2011;45(10):4645–51.
[55] US Department of Energy National Energy Technology Laboratory. Overview of DOE's gasification program. Technical report, 2010. <http://www.netl.doe.gov/technologies/coalpower/gasification/ref-shelf.html>.
[56] Kay SM. Fundamentals of statistical signal processing. Estimation theory, vol. I. New Jersey: Prentice Hall; 1993.